Supporting Materials for

A Novel 9-MC-3 and 15-MC-6 on-Set Stacked Metallacrown Single-Molelcule Magnet: Synthesis and Crystal Structure

Suna Wang[a,b], Lingqian Kong[c], Hua Yang[a], Zhoutong He[d], Zheng Jiang[d], Dacheng Li[*a], Suyuan Zeng[a], Meiju Niu[a], You Song[b]*, Jianmin Dou[*a]

a School of Chemistry and Chemical Engineering, Liaocheng University, 252059, Liaocheng
[b] State Key Laboratory of Coordination Chemistry, School of Chemistry and Chemical Engineering, Nanjing National Laboratory of Microstructures, Nanjing University, 210093, Nanjing, P. R. China
[c] Department of Chemistry and Biology, Dongchang College of Liaocheng University
[d] Shanghai Synchrotron Radiation Facility, 201204, Shanghai, P. R. China

* To whom correspondence should be addressed.

E-mail: jmdou@lcu.edu.cn (J.D.), yousong@nju.edu.cn (Y.S.). lidacheng@lcu.edu.cn (D. L.)

Experimental section

Materials and General Methods.

All chemicals and solvents were purchased commercially and used as received. All preparations and manipulations were performed under aerobic conditions. The melting points were obtained with Kofler micro melting point apparatus and uncorrected. Infrared-spectra were recorded on a Nicolet-5700 spectrophotometer using KBr discs and sodium chloride optics. The spectra were acquired at room temperature (298K) unless otherwise specified ; Elemental analyses were performed with a PE-2400II apparatus.

XAFS studies.

X-ray absorption fine spectroscopy (XAFS) was performed at Shanghai Synchrotron Radiation Facility (SSRF) on beam line 14W. A thin powder layer of these samples were prepared on a piece of Kapton tape for the measurement. All measurements were performed in a transmission mode. Linear background subtraction and normalization were performed using commercially available Athena software. Mn(II) and Mn(III) complexes were used to determine the valency of Mn of complex **1**. The former is Manganese(II) acetate tetrahydrate (Puratronic, 99.999% metal basis) purchased from Alfa-aesar, and the latter is a previously reported hexanuclear manganese(III) single-molecule magnet, $[Mn_6O_2(O_2CMe)_2(salox)_6(EtOH)_4]\cdot 4EtOH$ (H_2salox = salicylaldoxime). (Reference: Milios, C. J.; Raptopoulou, C. P.; Terzis, A.; Lloret, F.; Vicente, R.; Perlepes, S. P.; Escuer, A. *Angew. Chem. Int. Ed.* **2004**, *43*, 210.)

Synthesis of complex 1:

The preparation of the complex **1** is summarized in the following balanced chemical equation:

$$9Mn(O_2CMe)_2\cdot 4H_2O + 6Me\text{-}saoH_2 + 3MeOH + 2O_2 = [Mn_9O_4(Me\text{-}sao)_6(MeO)_3(O_2CMe)_3(MeOH)_2(OH)] + 15MeCOOH + 33H_2O$$

A methanol solution (10 mL) of $Mn(O_2CMe)_2\cdot 4H_2O$ (0.073 g, 0.30 mmol) was added dropwise to a dimethylformamide solution (10 mL) of Me-saoH$_2$ (0.045 g, 0.3 mmol). The resulting dark green solution was stirred for five hours. The filtrate was carefully layered with Et_2O and black rectangular crystals of the product were obtained two weeks later. Yield 65% (based on $Mn(O_2CMe)_2\cdot 4H_2O$). Elemental analysis (%): calcd for $C_{133}H_{173}Mn_{18}N_{17}O_{61}$, C 40.15, H 4.35, N 5.99; found: C 40.09, H 4.34, N 5.89; IR data (KBr pellet: cm^{-1}): 3431(vs), 2919(s), 2849(m), 1649(m), 1559(s), 1435(s), 1318(s), 1247(m), 1133(m), 1054(m), 978(s), 749(s), 673(s), 645(m), 552(m), 435(w).

Crystal Data for **1**: $C_{133}H_{173}Mn_{18}N_{17}O_{61}$, M = 3974.80, cubic, space group I23, a = 26.050(2), b = 26.050(2), c = 26.050(2) Å, V = 17677(3) Å^3, Z = 8, Dc = 1.356 g/cm^3, F(000) = 7312, crystal dimensions 0.13 × 0.11 × 0.11 mm, R1 = 0.0441, wR2 = 0.1080 for 2279 reflections with $I > 2\sigma(I)$, GOF = 1.097, largest peak/hole 0.66/-0.30. The lattice DMF molecules were also badly disordered, and the data were treated with the SQUEEZE option within PLATON which was used to calculate the solvent disorder area and remove its contribution to the overall intensity data (Reference: Spek, A. L. (2003), J. Appl. Cryst. 36, 7-13.).

Table S1. Selected bond distances and angles in complex **1**.

Mn(1)-O(5)	1.889(5)	Mn(1)-O(2)	1.902(5)
Mn(1)-O(1)	1.930(5)	Mn(1)-N(2)	1.987(6)
Mn(1)-O(6)	2.164(6)	Mn(1)-O(7)	2.422(5)
Mn(2)-O(4)	1.854(5)	Mn(2)-O(10A)	1.929(5)
Mn(2)-O(7)	1.939(5)	Mn(2)-N(1)	1.966(6)
Mn(2)-O(8)	2.138(6)	Mn(2)-O(2)	2.444(5)
Mn(3)-O(3)	1.891(5)	Mn(3)-O(7)	1.923(4)
Mn(3)-O(7B)	1.933(5)	Mn(3)-O(10)	1.954(5)
Mn(3)-O(9)	2.133(5)	Mn(3)-O(1)	2.525(5)
O(5)-Mn(1)-O(2)	170.3(3)	O(5)-Mn(1)-O(1)	90.48(16)
O(2)-Mn(1)-O(1)	94.2(2)	O(5)-Mn(1)-N(2)	87.65(18)
O(2)-Mn(1)-N(2)	86.2(2)	O(1)-Mn(1)-N(2)	169.4(2)
O(5)-Mn(1)-O(6)	94.8(3)	O(2)-Mn(1)-O(6)	93.4(2)
O(1)-Mn(1)-O(6)	92.9(2)	N(2)-Mn(1)-O(6)	97.6(2)
O(5)-Mn(1)-O(7)	90.5(3)	O(2)-Mn(1)-O(7)	82.08(19)
O(1)-Mn(1)-O(7)	78.86(18)	N(2)-Mn(1)-O(7)	90.7(2)
O(6)-Mn(1)-O(7)	170.2(2)	O(4)-Mn(2)-O(10A)	96.8(2)
O(4)-Mn(2)-O(7)	171.7(2)	O(10A)-Mn(2)-O(7)	79.93(19)
O(4)-Mn(2)-N(1)	90.9(2)	O(10A)-Mn(2)-N(1)	171.3(2)
O(7)-Mn(2)-N(1)	91.8(2)	O(4)-Mn(2)-O(8)	93.6(2)
O(10A)-Mn(2)-O(8)	91.6(2)	O(7)-Mn(2)-O(8)	94.2(2)
N(1)-Mn(2)-O(8)	91.8(2)	O(4)-Mn(2)-O(2)	91.7(2)
O(10A)-Mn(2)-O(2)	92.05(19)	O(7)-Mn(2)-O(2)	80.79(18)
N(1)-Mn(2)-O(2)	83.8(2)	O(8)-Mn(2)-O(2)	173.21(19)

Symmetry codes: A:-z+1, -x+1, y; B:-y+1, z, -x+1.

Figure S1. XAFS spectra of complex **1**, Mn(III) and Mn(II) complex. K edge position of complex 1 very near to that of Mn(III) complex indicates a +3 valence state.

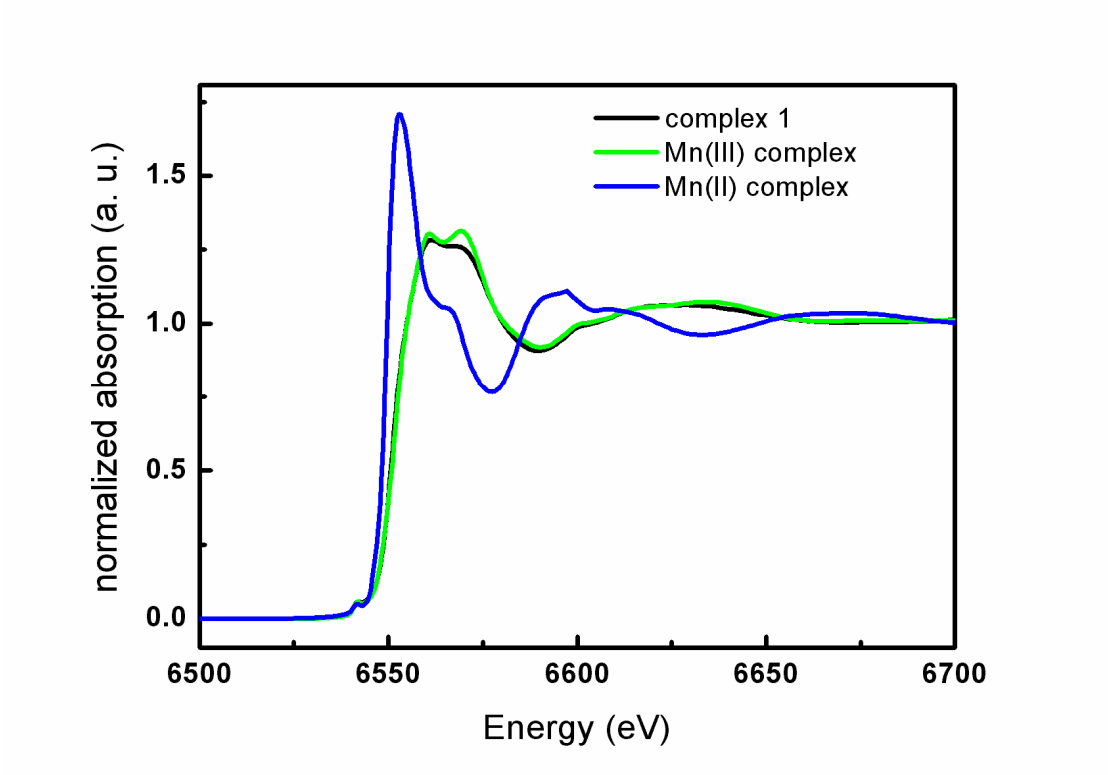

The attempt to reproduce the complex 1 spectra by a linear combination fit of references spectra Mn(III) and Mn(II), using standard fitting procedures in Athena (Reference: Ravel, B.; Newville, M.; *J. Synch. Rad.* 2005, 12, 537.), reveals a quantitative valence split only of 95.4±0.2% Mn(III) and 3.4±0.2% Mn(II).

Table S2. Bond Valence Calculations (BVS) for complex **1**.

Atom	+2	+3	+4
Mn1	3.322	3.063	3.005
Mn2	3.379	3.127	3.057
Mn3	3.313	3.055	2.964

Reference: Liu, W. T.; Thorp, H. H. *Inorg. Chem.* 1993, 32, 4102.

Figure S2. Plots of χ_M^{-1} *vs T* of **1** at 2 kOe field. The red solid line represents the best fit by the Curie-Weiss expression (in the temperature range of 50-300 K).

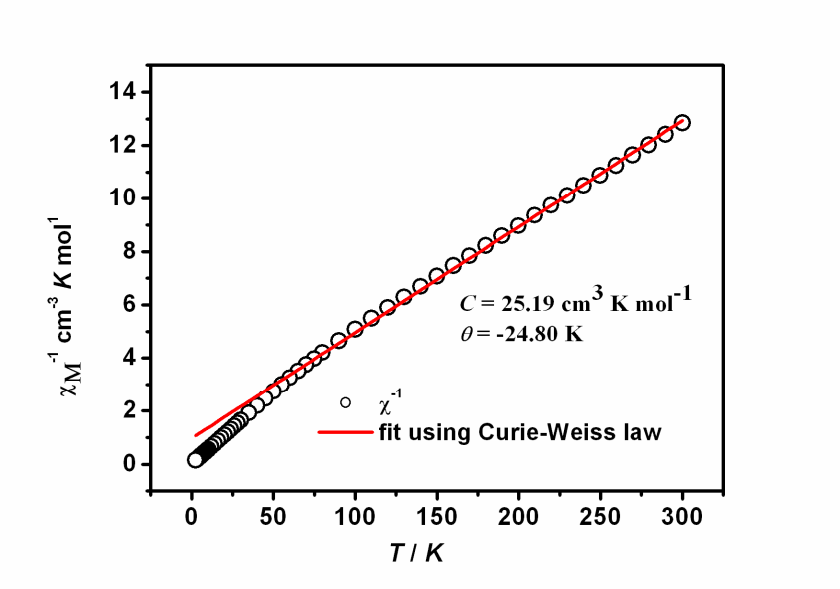

Figure S3. View of the connectivity and complicated magnetic exchange interactions between Mn(III) centers in complex **1**. Symmetry codes: A, 1-*z*, 1- *x*, *y*; B, +*y*, +*z*, +*x*.

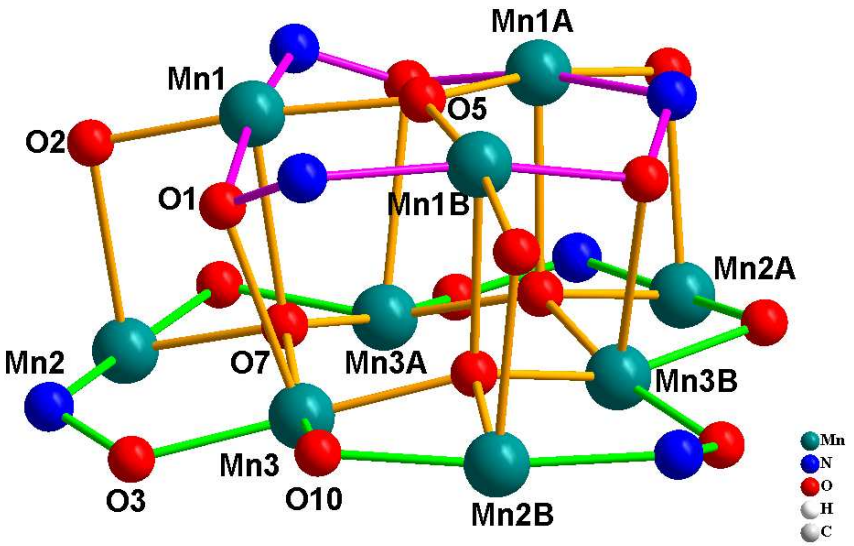

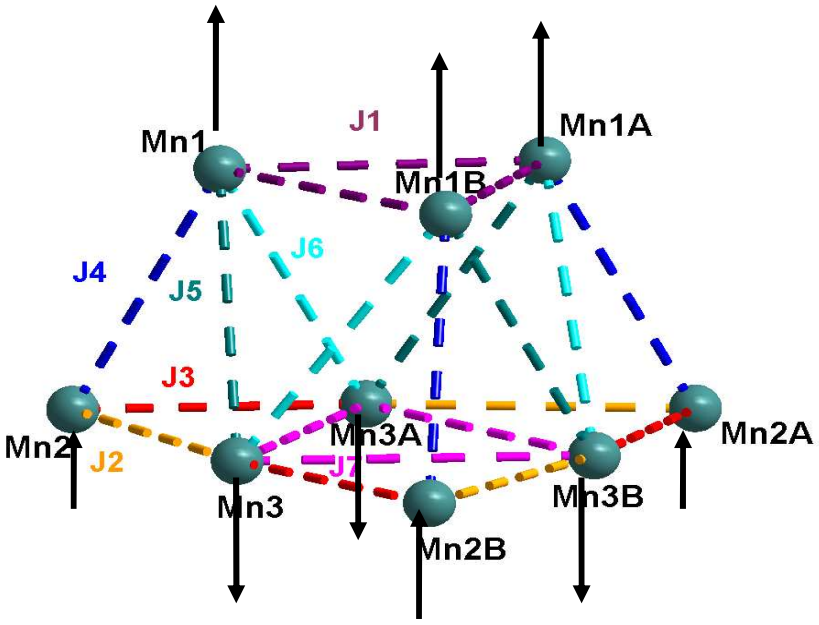

The Heisenberg Hamiltonian of **1** can be given as:

$$\hat{H} = -2J_1(\hat{S}_1\hat{S}_{1A} + \hat{S}_1\hat{S}_{1B} + \hat{S}_{1A}\hat{S}_{1B}) - 2J_2(\hat{S}_2\hat{S}_3 + \hat{S}_{2A}\hat{S}_{3A} + \hat{S}_{2B}\hat{S}_{3B})$$
$$- 2J_3(\hat{S}_2\hat{S}_{3A} + \hat{S}_{2B}\hat{S}_3 + \hat{S}_{2A}\hat{S}_{3B}) - 2J_4(\hat{S}_1\hat{S}_2 + \hat{S}_{1A}\hat{S}_{2A} + \hat{S}_{1B}\hat{S}_{2B})$$
$$- 2J_5(\hat{S}_1\hat{S}_3 + \hat{S}_{1A}\hat{S}_{3A} + \hat{S}_{1B}\hat{S}_{3B}) - 2J_6(\hat{S}_1\hat{S}_{3A} + \hat{S}_{1A}\hat{S}_{3B} + \hat{S}_{1B}\hat{S}_3)$$
$$- 2J_7(\hat{S}_3\hat{S}_{3A} + \hat{S}_3\hat{S}_{3B} + \hat{S}_{3A}\hat{S}_{3B})$$

Due to the large Jahn-Teller effect with long Mn-O distance (Mn1-O7, 2.422(5) Å; Mn2-O2, 2.444(5) Å; Mn3-O1, 2.525(5) Å), the magnetic exchange interactions between the metal centers on the equatorial planes may have larger influences than those at the apical axes. According to the references, **torsion angles of Mn-N-O-Mn above 31.4°always lead to ferromagnetic properties** (References: (a) Milios, C. J.; Raptopoulou, C. P.; Terzis, A.; Lloret, F.; Vicente, R.; Perlepes, S. P.; Escuer, A. *Angew. Chem. Int. Ed.* **2004**, *43*, 210; (b) Milios, C. J.; Vinslava, A.; Wood, A. P.; Parsons, S.; Wernsdorfer, W.; Christou, G.; Perlepes, S. P.; Brechin, E. K. *J. Am. Chem. Soc.*, **2007**, *129*, 8; (c) Prescimone, A.; Milios, C. J.; Moggach, S.; Warren, J. E.; Lennie, A. R.; Sanchez-Benitez, J.; Kamenev, K.; Bircher, R.; Murrie, M.; Parsons, S.; Brechin, E. K. *Angew. Chem. Int. Ed*. **2008**, *47*, 2828; (d) Feng, P. L.; Stephenson, C. J.; Amjad, A.; Ogawa, G.; Barco, E.; Hendrickson, D. H. *Inorg. Chem*. **2010**, *49*, 1304.). **As a result, in complex 1, ferromagnetic exchange interactions exist in the severe twisting of the Mn-N-O-Mn moieties (43.7°) of 9-MC-3 core (J_1>0). In the 15-MC-6 core, however, the small torsion angles (25.2°) of the Mn-N-O-Mn moieties lead to antiferromagnetic exchange interactions between the Mn ions (J_2<0). For Mn-O-Mn bridges, Mn-O-Mn angles smaller than about 102° always lead to ferromagnetic interactions** (Reference: Feng, Y. H.; Wang, C.; Zhao, Y. F.; Liao, D. Z.; Yan, S. P.; Wang, Q. L. *Inorg. Chim. Acta.* **2009**, *362*, 3563 and references therein.). **Thus, ferromagnetic interactions between Mn2 and Mn3A (J_3>0). The resulting total spin of S = 6 ([3×2+(3×2-3×2)]), consistent with both dc and ac magnetic measurements.** For multiple bridges, the exchange interactions should also be the overall interactions of all the bridges. For Mn1···Mn2, two Mn-O-Mn anlges (Mn1-O2-Mn2 and Mn1-O7-Mn2) are both smaller than 102°, which may lead to ferromagnetic interactions (J_4>0). For Mn1···Mn3, of the two Mn-O-Mn angles, Mn1-O1-Mn3, 99.0°; Mn1-O7-Mn3, 102.8°), one may lead to ferromagnetic interactions while the other antiferromagnetic interactions. Considering the weaker

interactions at the apical positions than those in equatorial plane, antiferromagnetic interactions (J_5<0) may be assigned. Detailed magnetic exchanges for the Mn-O-Mn bridges are listed in the table below.

connectivity	angle(°)	Magnetic exchange
Mn1-N2-O1-Mn1A	43.7	J_1>0
Mn2-N1-O3-Mn3	25.2	J_2<0
Mn2-O10-Mn3A	97.0	J_3>0
Mn2-O7-Mn3A	97.4	
Mn1-O2-Mn2	98.5	J_4>0
Mn1-O7-Mn2	98.3	
Mn1-O1-Mn3	99.0	J_5<0
Mn1-O7-Mn3	102.8	
Mn1-O7-Mn3A	107.4	J_6<0
Mn3-O7-Mn3A	132.9	J_7>0

Figure S4. Plots of the in-phase (χ_M') signals and $\chi_M'T$ versus temperature of **1** in ac susceptibility studies in zero applied static field with an oscillating field of 5.0 Oe at the indicated frequencies.

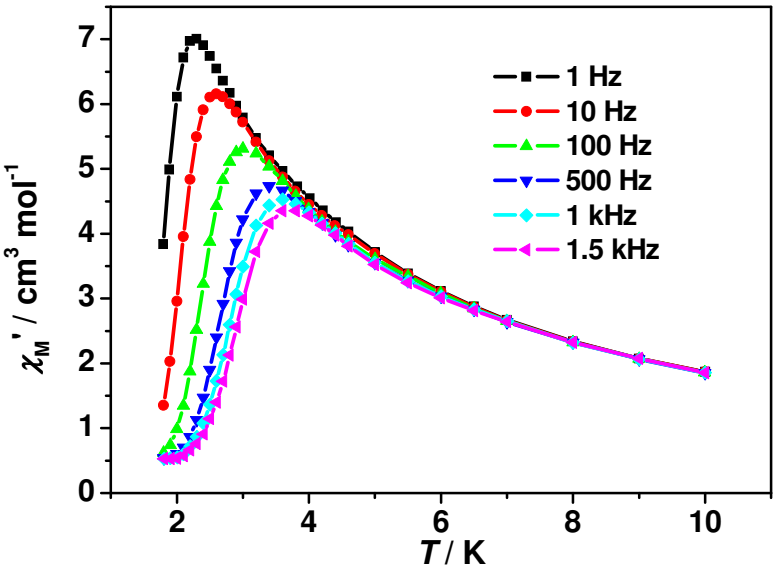

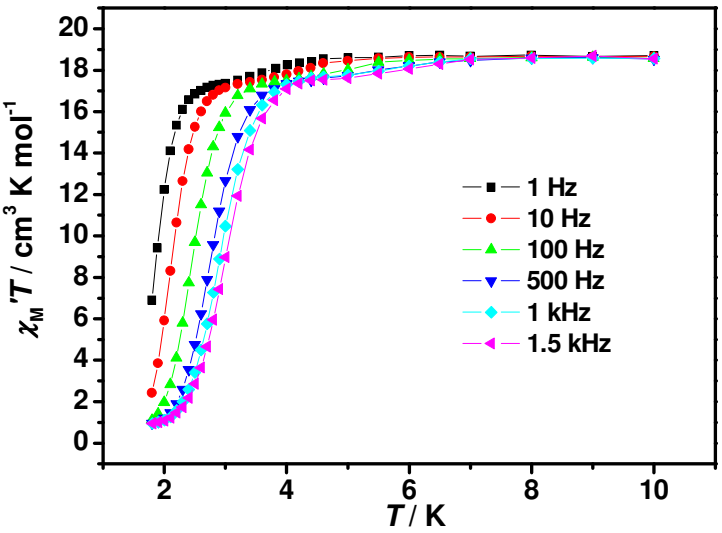

Figure S5. Plots of T_B^{-1} versus ln(2πf) for Arrhénius fit.